

The FASEB Journal express article 10.1096/fj.05-3778fje. Published online October 6, 2005.

Key gravity-sensitive signaling pathways drive T-cell activation

J. B. Boonyaratanakornkit,^{*,†} A. Cogoli,[‡] C.-F. Li,[§] T. Schopper,[‡] P. Pippia,^{||} G. Galleri,^{||} M. A. Meloni,^{||} and M. Hughes-Fulford^{*,†,§,¶}

^{*}Laboratory of Cell Growth, Veterans Affairs Medical Center, San Francisco, California 94121;

[†]University of California San Francisco School of Medicine, San Francisco, California 94143;

[‡]Swiss Federal Institute of Technology, 8005 Zurich, Switzerland; [§]Laboratory of Cell Growth, Northern California Institute for Research and Education, San Francisco, California 94121;

^{||}Department of Physiological, Biochemical, and Cellular Sciences, University of Sassari, I-07100 Sassari, Italy; and [¶]Laboratory of Cell Growth, University of California San Francisco, San Francisco, California 94143

Corresponding author: Millie Hughes-Fulford, Ph.D., Director, Laboratory of Cell Growth, University of California, Department of Medicine and Veterans Affairs Medical Center, 4150 Clement Street, MC151F, San Francisco, CA 94121. E-mail: millie.hughes-fulford@med.va.gov

ABSTRACT

Returning astronauts have experienced altered immune function and increased vulnerability to infection during spaceflights dating back to Apollo and Skylab. Lack of immune response in microgravity occurs at the cellular level. We analyzed differential gene expression to find gravity-dependent genes and pathways. We found inhibited induction of 91 genes in the simulated freefall environment of the random positioning machine. Altered induction of 10 genes regulated by key signaling pathways was verified using real-time RT-PCR. We discovered that impaired induction of early genes regulated primarily by transcription factors NF- κ B, CREB, ELK, AP-1, and STAT after crosslinking the T-cell receptor contributes to T-cell dysfunction in altered gravity environments. We have previously shown that PKA and PKC are key early regulators in T-cell activation. Since the majority of the genes were regulated by NF- κ B, CREB, and AP-1, we studied the pathways that regulated these transcription factors. We found that the PKA pathway was down-regulated in *vg*. In contrast, PI3-K, PKC, and its upstream regulator pLAT were not significantly down-regulated by vectorless gravity. Since NF- κ B, AP-1, and CREB are all regulated by PKA and are transcription factors predicted by microarray analysis to be involved in the altered gene expression in vectorless gravity, the data suggest that PKA is a key player in the loss of T-cell activation in altered gravity.

Key words: immune response • gene expression • signal transduction • microarray • microgravity

In 1973, NASA launched the Skylab Space Station, and subsequent analysis of blood drawn from primary and backup crews before launch and postflight gave rise to the first evidence of altered immune function in space. Lymphocyte response to mitogen treatment was normal during preflight and in backup crews but was significantly reduced in blood from the nine returning Skylab astronauts (1). The relatively high incidence of infection observed in Apollo astronauts inflight and 1 wk postflight was an impetus for increased efforts to study the immune system in Skylab (1). Correlations with elevated cortisol levels and sympathetic activation detected in blood and urine samples from astronauts led early investigators to propose a whole-body theory and attribute impaired immunity in space to the endocrine system (1, 2). However, in 1983, Cogoli et al. (3-5) demonstrated with isolated lymphocyte experiments a 90% reduction in lymphocyte activation in microgravity with no significant change in glucose uptake or utilization. Later fluorescent microscopy studies by Cogoli (6) then showed no significant reduction in membrane bound concanavalin A (Con A) in microgravity. Subsequent experiments on human and mouse lymphocytes revealed a significant decrease in IL2 and IL2R α synthesis and a reduction in proliferation (6, 7). Lewis et al. (5) and Hughes-Fulford (8) then demonstrated that spaceflight leads to anomalous cytoskeletal organization and diffusive microtubule organizing centers. Taken together, these findings pointed to a cellular based dysfunction and a significant role for gravity in the immune response. We hypothesized that depressed immune function is most likely due to reduced expression of early genes key in initiating and maintaining T-cell activity. Utilization of a random positioning machine (RPM) and Affymetrix GeneChip[®] technology allowed us to ascertain key gravity-dependent gene expression patterns and signaling pathways involved in the human immune response. Despite the presence of a gravitational field 160 miles above Earth, humans onboard orbiting spacecrafts or stations experience $\sim 10^{-4}$ g because orbital velocities generate a vectorless gravity (vg) environment (9). By continually altering the terrestrial 1 g vector, the RPM generates a low-shear vg environment with residual centripetal force of 10^{-3} g through random three-dimensional rotation to approximate the effects of true freefall or microgravity found on the shuttle (9–11). Considering that all terrestrial life evolved in a 1 g field, it is not surprising to find that certain cell types and cellular pathways require the gravity of Earth for normal function. By identifying the specific genes that undergo statistically significant early transcriptional induction in terrestrial gravity but not in vg, we were able to narrow our search for major regulatory signal transduction pathways and found that PKA plays a key role in gravity modulation of T-cell activation in vg.

MATERIALS AND METHODS

T-cell isolation, culture, and activation

Peripheral blood leukocytes of three human donors were isolated from blood bank buffy-coats (Red Cross, Zurich, Switzerland) by Ficoll-Hypaque density gradient centrifugation, and T cells were purified using high affinity CD3⁺ T-cell enrichment columns (R&D Systems, Minneapolis, MN). The cells were resuspended in RPMI-1640 with 10% FCS at 3–8 million cells/ml. A portion of T cells was activated with a final concentration of 5 μ g/ml Con A (Sigma, St. Louis, MO) with 4 μ g/ml anti-CD28 antibody (PharMingen, San Diego, CA) and incubated for 4 h at 1 g or loaded onto a RPM (Dutch Space, Leiden, Netherlands) rotating at 60°/s at 37°C with unactivated controls. Random rotation at 60°/s, 1 or 3 cm away from the center of rotation yields gravity contours from 1×10^{-3} to 2×10^{-3} g as calculated by $g' = \omega^2 R / g_0$ where $g_0 = 9.81 \text{ m/s}^2$, ω

= 1.0 radian/s, and $r = 0.01$ or 0.03 m (11, 12). T cells on the RPM were conditioned for 2 h before collection or activation to allow the cells to equilibrate to the vg environment.

RNA extraction and cleanup

RNA was isolated using guanidinium isothiocyanate as described previously (13). RNA cleanup was performed using RNeasy[®] MinElute columns (Qiagen, Valencia, CA). RNA concentration and purity were determined from measuring absorbance at 260 and 280 nm with a GeneQuant (Pfizer, New York, NY); 0.3 μg total RNA was run on a 1% denaturing gel, or 100 ng total RNA were loaded on the 2100 Bioanalyzer (Agilent, Palo Alto, CA) to verify RNA integrity.

Microarray sample preparation

The Human Genome Focus Array (Affymetrix, Santa Clara, CA) is composed of 8,796 probe sets corresponding to well-annotated genes from the NCBI RefSeq database; 1.8 μg of total RNA were aliquoted for first and second strand cDNA synthesis using a HPLC purified oligo-(dT) primer (Affymetrix) and 200 U SuperScript[™] II reverse transcriptase (Invitrogen, Carlsbad, CA). Ten microliters of the cDNA were then aliquoted for in vitro transcription and biotin labeling using the BioArray[™] high yield[™] RNA transcription labeling kit (Enzo, New York, NY). The reaction was incubated for 10 h at 37°C. After cRNA fragmentation, the samples were transported to the Gladstone Institute Genomics Core. Ten micrograms of the labeled cRNA were hybridized at a final concentration of 0.05 $\mu\text{g}/\mu\text{l}$ onto Focus arrays at 45°C for 16 h. The arrays were stained using a Fluidics Station 400 (Affymetrix) and scanned using a GeneArray[®] Scanner (Affymetrix).

Microarray data analysis and gene selection

Before analysis, several internal parameters from each Affymetrix GeneChip[®] were checked to verify sample and array quality such as noise and background levels, present calls, and 3'/5' ratios as described at http://www.affymetrix.com/support/downloads/manuals/data_analysis_fundamentals_manual.pdf. After background subtraction and image processing in Affymetrix Microarray Suite (MAS) 5.0, data normalization was performed in GeneSpring[®] 6.2 (Silicon Genetics, Redwood City, CA). Total intensity normalization to the median was employed to adjust for differences in labeling and the quantity of initial total RNA (14, 15, 16).

Significant differential gene expression was identified after scaling each gene to its corresponding signal in the 1 g 0 h baseline to derive expression ratios. Only genes flagged with a present call in at least one array were considered for subsequent analysis. To focus on genes normally induced by mitogen, a twofold upregulation cutoff at 1 g 4 h was established. In addition to the ad hoc fold change and detection call selection criteria, a paired two-tailed t test between 1 g 0 h and 1 g 4 h samples was implemented, and a two-way ANOVA was applied to identify significant differential gene expression patterns resulting from a gravity, treatment, or interaction effect (17). The cutoff for significance was set at $P \leq 0.05$, and all parametric tests were performed on the logarithm of expression ratios. Notably, in our previous study on T-cell signal transduction in only normal gravity, the two-way ANOVA was not applicable (18). Hierarchical clustering was applied using a centered Pearson correlation as the distance metric (12, 16, 19). The TRANSFAC[®] database and MATCH[™] program (Biobase, Wolfenbüttel,

Germany) were used to identify potential regulatory sequences 1000 nucleotides upstream of the transcription start site (20). Upstream sequences were attained from the UCSC Genome Browser at <http://genome.ucsc.edu>. A description of our microarray experiment is posted on the Gene Expression Omnibus found at <http://www.ncbi.nlm.nih.gov/geo>. The platform accession number is GPL201; sample accession numbers are GSM24817, GSM29564, GSM29565, GSM29566, GSM29567, GSM29568, GSM29569, GSM29570, GSM29571, GSM29572, GSM29573, and GSM29574; and series accession number is GSE1709.

Quantitative real-time RT-PCR

To verify data obtained from microarray analysis, real-time RT-PCR was performed on 10 genes. Gene specific primers for an 18S internal control (Ambion, Austin, TX) and *CSF2*, *IFNG*, *IL2*, *IL2RA*, *LTA*, *MIF*, *NFKB1*, *STAT1*, *TNF*, and *XCL2*, designed using Oligo[®] 6.0 software (Molecular Biology Insights, Cascade, CO) and synthesized by Qiagen, were used to perform quantitative PCR. An equivalent of 0.05 µg total RNA was reverse transcribed for each PCR reaction (13). The ABI Prism[®] 7900HT (Applied Biosystems, Foster City, CA) was used to quantify RNA amounts represented by SYBR[®] Green fluorescence with the comparative threshold cycle number method. The Eq. $2^{\Delta\Delta C_T}$ was computed to obtain expression ratios normalized to the 18S internal control (21).

Transcription factor immunoblot analysis

Cells were lysed 30 min after the addition of mitogen, using lysis buffer as described previously (22). Membranes were probed with anti-phospho-CREB (Ser133) antibody (Upstate, Charlottesville, VA), anti-phospho-LAT (Tyr171) antibody (Cell Signaling Technology, Beverly, MA), and anti-phospho-PI3-K (Tyr508) antibody (Santa Cruz Biotechnology, Santa Cruz, CA). Proteins were detected by enhanced chemiluminescence (Pierce, Rockford, IL) and exposed on autoradiography film. Films were scanned and bands quantified with UNSCANIT[®] densitometry software (Silk Scientific, Orem, UT).

RESULTS

Gravity regulates the distribution of global gene expression in T cells during activation

T cells isolated from three humans were activated at 1 g or on the RPM in a vg environment. Using microarray-based expression profiling, we assessed global gene expression from unactivated T cells (1 g 0 h and vg 0 h) and T cells treated with Con A and anti-CD28 antibody (1 g 4 h and vg 4 h). The T cells exhibited significant changes in gene expression distribution only after activation in normal gravity ([Fig. 1A](#)). Ninety-nine genes were significantly up-regulated above twofold after activation at 1 g ([Fig. 1B](#)). Untreated cells in vg showed little or no change in expression distribution ([Fig. 1C](#) and [D](#)). T cells treated with mitogen in a vg environment had a compressed distribution and a drastic drop in gene induction ([Fig. 1E](#)). Notably, only 9 of the 99 genes passed our criteria for significant up-regulation on the RPM at 4 h, and, even then, induction of 8 of the genes was comparatively reduced ([Fig. 1F](#)).

Cluster analysis of genes differentially expressed during T-cell activation in normal and vg

The 99 genes significantly up-regulated by activation in normal gravity were clustered hierarchically to permit a visual examination of gene expression patterns, function, and regulation ([Fig. 2A](#)). Cluster A was comprised of 16 genes that were the most highly upregulated after activation in 1 g but were not induced by mitogen on the RPM. Several cytokines and their related genes, including *IL2*, *IL1*, and *IFNG*, were grouped in cluster A. The expression of 18 genes in cluster B also increased, but to a lesser extent, after activation in 1 g. The chemokines *CCL3*, *CCL4*, and *CCL20* were grouped in cluster B. Both clusters A and B exhibited a relatively smaller increase in expression in the untreated RPM samples.

The expression of 12 genes in cluster C increased after activation in 1 g, did not change in untreated vg samples, and decreased 4 h after the addition of mitogen to the vg samples. Cluster D was comprised of 14 genes and cluster E was comprised of 33 genes that were up-regulated after activation in 1 g but remained relatively static before and after activation in vg. Finally, cluster F contained six genes that were up-regulated after activation in 1 g and vg.

The sample profiles illustrate that 99 genes predominantly exhibited significant up-regulation during activation in 1 g but little change or down-regulation of gene expression in vg. This relationship was examined mathematically by principal component analysis (PCA) of each sample profile ([Fig. 2B](#)). PCA is used to identify patterns within complex datasets by reducing the effective dimensionality of gene expression space. For instance, here, the 99-dimensional space corresponding to the 99 significant genes is projected onto a readily visualized two-dimensional plot providing a simplified view of the separation of the data into distinct groups (14, 23). Unactivated T-cell samples cultured in normal gravity clustered into one class in the fourth quadrant of the plot. The untreated and treated T cells in vg clustered together into another class in the third quadrant. Activated T cells cultured in normal gravity clustered into a separate class in the second quadrant. Based on our results from PCA, the gene expression signatures in different gravity and treatment conditions were distinct.

Early T-cell signaling through key transcription factors is impaired in vg

After cluster analysis, gene ontologies and the literature were used to classify the genes by their biological or molecular function ([Table 1](#)). The normalized expression ratios represent the average from three independent donors at each condition. The most highly differentially expressed genes encoded cytokines, chemokines, and members of the tumor necrosis factor superfamily. The genes that were significantly induced by mitogen in 1 g were grouped by common regulatory binding sites or pathway involvement as determined by performing a literature search and using the MatchTM program on the TRANSFAC[®] database to identify key signaling cassettes involved in T-cell activation ([Fig. 3A](#)). Twenty-eight percent of the significantly induced genes were either a component of the NF- κ B signaling pathway, contained computed NF- κ B binding sites in the promoter, or had experimental evidence for transcriptional regulation by NF- κ B. Every gene in this group, except *OAS3*, was suppressed in vg.

Real-time RT-PCR confirms that early gene induction is suppressed in a vg environment

The quantitative real-time PCR results yielded expression profiles similar to those obtained from microarray analysis. The real-time PCR results validated the early gene induction in 1 g, and suppression in vg, of representative genes regulated by major signaling pathways, including *IFNG*, *XCL2*, *IL2RA*, *IL2*, *CSF2*, *STAT1*, *LTA*, *TNFA*, *MIF*, and *NFKB1* (Fig. 3B). To examine preprocessing effects on microarray data analysis, the mean normalized expression ratios preprocessed by three methodologies dChip, Robust Multi-chip Analysis (RMA), and MAS were compared with mean normalized band intensities from semi-quantitative RT-PCR for the three donors (Fig. 4; 15, 24). The expression profiles for the cytokines *IFNG* and *IL2* and the receptor subunits *IL2RA*, *IL2RB*, and *IL2RG* generated from microarray analysis and semi-quantitative RT-PCR were similar. Although the immune response to activation for each of these five genes differed in magnitude between donors, the expression profiles followed similar trends across donors. Significant up-regulation of *IFNG* and *IL2RA* at 1 g 4 h was observed with respect to 1 g 0 h from RT-PCR data and from all three microarray preprocessing methods. Significant up-regulation of *IL2* expression was also detected in the RT-PCR data and after preprocessing in MAS and dChip.

CREB transcription factor activation occurs in 1 g but not in vg

To further validate the gene expression analysis, we performed immunoblots against phosphorylated CREB. T-cells activated with Con A and anti-CD28 antibody for 30 min at 1 g showed significant up-regulation of CREB phosphorylation compared with 1 g controls (Fig. 5A). In contrast, the activation of CREB by phosphorylation failed to occur in T cells treated with mitogen in vg. The protein abundance of activated CREB was significantly different between the treated 1 g and vg samples.

LAT adaptor protein is comparably activated in both 1 g and vg

To investigate PKC signaling pathway involvement, we performed immunoblots against phosphorylated linker of activation in T cells (LAT), an upstream adaptor protein that activates the PKC pathway. We found that LAT phosphorylation occurred at significant levels after T cells were incubated with Con A and anti-CD28 antibody for 30 min in both 1 g and vg compared with unactivated controls (Fig. 5B). No significant differences were detected in phosphorylation levels in samples treated at vg compared with samples activated at 1 g. Moreover, the phosphorylation of PI3-K was not down-regulated in vg (Fig. 5C). We also found that the phosphorylation of PKC was not down-regulated in vg (data not shown).

DISCUSSION

Astronauts represent a unique population exposed to extreme environmental factors never before experienced by humans; 15 of 29 Apollo astronauts reported bacterial or viral infection during, immediately after, or within 1 wk of landing back on Earth (25). Apollo 7 marked humanity's first experience with spaceflight infection when all three crewmembers contracted head colds during their mission (25). On Apollo 13, one astronaut contracted *Pseudomonas aeruginosa* and suffered from intense chills and fever (25). *P. aeruginosa* is an opportunistic pathogen and rarely causes disease unless the person suffers from a break in epithelia or from immune suppression.

After Apollo 13, NASA recognized the potential hazard of exposure to communicable disease before flight and the subsequent manifestation of symptoms during flight. As a result, NASA implemented a preflight quarantine program that subsequently reduced the number of reported infections to one Apollo astronaut (25).

Immune suppression in the absence of gravity poses a novel barrier to the early immune response. Using microarray analysis, we found that 99 genes were significantly up-regulated during early T-cell activation in normal gravity. However, when we removed the gravity vector, the majority of those genes showed no significant mitogen induced gene expression. The data presented here suggest that gravity is a key regulator of the cell-mediated immune response and that its absence either slows, impedes, or fully blocks signaling pathways essential for early T-cell activation. In vg, suppression of transcriptional induction encompasses numerous signaling pathways essential to T-cell activation. Expression of downstream targets of signal transduction cascades, including genes involved in proliferation, apoptosis, biosynthesis, and secretion, is repressed in the absence of gravity. A variety of signals are responsible for conveying an external stimulus to elicit a cellular response to mitogen (Fig. 6). The T-cell receptor and CD28 initiate signal transduction pathways that induce the majority of the genes identified here by microarray analysis.

Microscopy studies of T cells after automated injection of fluorescent labeled Con A in sounding rocket flight by Dr. Cogoli's group (6, 26) clearly demonstrated that Con A binding to the T-cell receptor (TCR) is not influenced by microgravity. We have shown, here, that the NF- κ B, CREB, ELK, AP-1, and STAT pathways exert transcriptional control over the majority, or 59%, of significantly induced genes (Fig. 3A). Furthermore, as seen in Fig. 6, NF- κ B, CREB, ELK, and AP-1 can share subsets of the same upstream kinases to cross-talk with one another and achieve gene induction in the nucleus (18). It is noteworthy that mechanical stimuli activate these same pathways (27). Moreover, kinase activities require the successful formation of signaling complexes at cholesterol-rich lipid rafts for successful propagation of signals away from the antigen receptor (28, 29). Thus, since fluorescent microscopy has shown that normal receptor cross-linking occurs in microgravity, we thought it highly likely that an early alteration in signaling components downstream of cross-linking the antigen receptor and at or upstream of PKC activation during assembly of the signaling complex at lipid rafts occurs before the signal can propagate and diverge into distal pathways thereby simultaneously precluding activation of multiple transcription factors, like NF- κ B, CREB, and AP-1, in vg (Fig. 6). We found, however, that phosphorylation of both PKC and its upstream regulator LAT were not down-regulated in vg.

The details of the signal transduction events leading from early TCR and CD28 activation to expression of IL2, IFN γ , and the IL2R subunits have not been fully elucidated until recently. Our group has published new data characterizing the cross-talk between the NF- κ B, CREB, ELK, and AP-1 signaling pathways highlighted here as responsible for impaired activation in altered gravity (18). We demonstrated a sequence of events in which IL2 transcription is turned on first within 2 h, followed by IL2R α within 4 h. Addition of PKC and PKA inhibitors in the presence of Con A and anti-CD28 significantly blocked IFN γ , IL2, and IL2R α gene induction. T-cells with a PKA regulatory subunit knocked out also exhibited transcriptional suppression. In both cases, IL2R β and IL2R γ expression was unaffected. These findings using small molecule

inhibitors parallel the data presented whereby the RPM environment blocked IFN γ , IL2, and IL2R α gene induction without affecting IL2R β and IL2R γ expression.

NF- κ B and CREB were the top two transcription factors predicted by microarray analysis to be involved in gravity-mediated gene expression. Since the PKA signaling pathway regulates these transcription factors, we thought that PKA signaling could be affected by vg. In early activation, CREB is phosphorylated within 30 min which was inhibited by PKC inhibitor and completely blocked by PKA inhibitor (18). Here, we report that the activation of CREB by phosphorylation within 30 min was significantly blocked by a vg environment (Fig. 5A). The loss of CREB phosphorylation implicates a failure of the PKA signal transduction pathway during T-cell exposure to mitogen in vg. It is notable that PKA has been shown to be intricately involved in activating NF- κ B in addition to CREB (30). The PKA catalytic subunit is associated with the I κ B and NF- κ B complex (30). In this complex, PKA is inactive, but when inducers of NF- κ B are added, I κ B is degraded and PKA phosphorylates NF- κ B p65 at a consensus sequence leading to a dramatic increase in NF- κ B transcriptional activity and enhanced DNA binding (30–33). Furthermore, when PKA is inhibited with H-89, NF- κ B activity and nuclear translocation are inhibited (30). PKA may have a central role interconnecting CREB and NF- κ B needed during early induction of gene expression in normal gravity. We also looked at the activation of PKC and PI3-K signaling pathways as well as LAT, an upstream activator of PLC γ and, subsequently, PKC. LAT is phosphorylated by 30 min after mitogen exposure and LAT phosphorylation was not affected by vg (Fig. 5B). We also found that PKC phosphorylation is intact in vg (data not shown). Moreover, we did not detect any significant changes in PI3-K phosphorylation at either 1 g or vg by 30 min (Fig. 5C).

Gene expression of two key cytokines *CSF2* and *IL2*, after mitogen treatment in vg, was reduced 98 and 92%, respectively, compared with activated samples at 1 g (Table 1). *CSF2* gene induction is responsible for promoting the production, differentiation, and function of granulocytes and macrophages during a response to infection (34). *IL2* drives T-cell proliferation and differentiation into armed effector cells (35). In addition, induction of *IL2RA*, a marker of T-cell activation, was observed in 1 g but not in vg. Upon activation, T cells begin transcription and synthesis of the α subunit to form a high-affinity heterotrimeric receptor to trigger growth, proliferation, and differentiation (36). The presence of *IL2* normally promotes *IL2RA* transcription, yet exogenous *IL2* still fails to restore T-cell activation in microgravity (37). Similar trends in *IL2* and *IL2R α* protein expression were observed from Spacelab flight experiments (37). This supports our hypothesis that intracellular signaling pathways integral to lymphocyte activity are not fully functional in vg. The failure to induce cytokine and receptor synthesis likely contributes to the loss in the adaptive immune system's capacity to fight infection and disease in vg.

The chemokines *XCL1*, *XCL2*, *CCL3*, *CCL4*, *CCL20*, and *CXCL10* had the highest magnitudes of up-regulation during 1 g activation, ranging from 7.8- to 252-fold (Table 1). Their drastic loss of induction in vg may contribute to an inhibition of lymphocyte trafficking (9). *XCL1* regulates T-cell migration by binding to its chemokine receptor and is induced during CD28 costimulation along with *CCL3* and *CCL4* (38). The lack of chemokine gene induction in vg may imply that signaling from CD28 is blocked despite crosslinking by anti-CD28 antibody (Fig. 6).

We discovered that five genes of the tumor necrosis factor superfamily *TNF*, *LTA*, *TNFSF14*, *TNFRSF6*, and *TNFRSF9* were suppressed in vg, with expression ratios from treated vg samples ranging from 4 to 48% of the ratios at 1 g. These functionally related genes were grouped together with *NFKB1* in cluster E (Fig. 2A). These genes exhibited similar expression profiles and appear to be coregulated, and they either lead to NF- κ B activation or are transcriptionally regulated by NF- κ B (Fig. 6) (39-43). Expression profiling revealed that the gene *BCL2A1* was induced during early T-cell activation only at 1 g. NF- κ B-dependent induction of *BCL2A1* expression has been shown to be essential to cell survival after lymphocyte activation by suppressing apoptosis (44).

In vg, we found that peripheral blood T-cells fail to achieve the expression profiles characteristic of normal activation and differentiation. However, it is important to note that our findings should not be broadly extrapolated to other biological systems since gravity-mediated regulation of signal transduction and gene expression is cell-type specific (9). For example, single cell organisms, like bacteria, grow faster and exhibit enhanced antimicrobial resistance on the Space Shuttle (45).

Our immune system protects us from infection and disease, yet T cells lose their adaptability in spaceflight. This study builds and extends on earlier discoveries that immune suppression is a factual phenomenon of manned space travel. The physical mechanisms by which the T cell responds to gravity remain an intriguing enigma and the Space Shuttle and International Space Station offer abundant opportunities for both in vitro and in vivo studies. We have identified the genes induced during a normal immune response and have shown that it is highly likely that alterations in signal transduction and transcription factor induction preclude full T-cell activation in vg. We also show that PKA signal transduction is down-regulated in vg while the PI3-K, PKC and pLAT signals are not inhibited. The genes identified and classified in this study can serve as a springboard for further investigations into immune function in normal and altered gravity. Such studies will advance our understanding of the human immune system in health and disease and give us insight into, and an appreciation for, the fundamental biological laws governing Earth's gravity-based life.

ACKNOWLEDGMENTS

This work was supported by a collaboration between NASA and the PRODEX program of the European Space Agency. The NASA portion was supported by grants NCC-2-1361 and NAG-2-1286 in the Laboratory of Cell Growth, NCIRE, and a Department of Veterans Affairs Merit Review, VAMC, San Francisco. The ESA portion was supported by Contract 13634/NL/VJ (IC) to ETH Zürich, Switzerland. Scientific Heading: Immunobiology. The General Clinical Research Center Core Genomics Laboratory operating under grant number M01RR00083-42 at the San Francisco General Hospital provided microarray hybridization support. Many thanks to R. Beatty, J. Hatton, S. Sayyah, E. Sugano, and E. Warren for extraordinary support and advice, S. Dugdale for graphic design, and C. Barker, D. Erle, and C. Griffin for invaluable expertise in microarray technology. We dedicate this project to the crew of STS107 for pursuing a courageous mission to explore, to discover, and to boldly go where no one has gone before.

REFERENCES

1. Kimzey, S. L. (1977) Hematology and immunology studies. In *Biomedical results from Skylab* (Johnson, R. S., and Dietlein, L. F., eds) pp. 248–282, NASA, Washington, DC
2. Leach, C. S., and Rambaut, P. C. (1977) Biochemical responses of the Skylab crewmen: an overview. In *Biomedical results from Skylab* (Johnson, R. S., and Dietlein, L. F., eds) pp. 204–216, NASA, Washington, DC
3. Cogoli, A., Bechler, B., Cogoli-Greuter, M., Criswell, S. B., Joller, H., Joller, P., Hunzinger, E., and Muller, O. (1993) Mitogenic signal transduction in T lymphocytes in microgravity. *J. Leukoc. Biol.* **53**, 569–575
4. Cogoli, A., Tschopp, A., and Fuchs-Bislin, P. (1984) Cell sensitivity to gravity. *Science* **225**, 228–230
5. Lewis, M. L., Reynolds, J. L., Cubano, L. A., Hatton, J. P., Lawless, B. D., and Piepmeier, E. H. (1998) Spaceflight alters microtubules and increases apoptosis in human lymphocytes (Jurkat). *FASEB J.* **12**, 1007–1018
6. Cogoli, A. (1997) Signal transduction in T lymphocytes in microgravity. *Gravit. Space Biol. Bull.* **10**, 5–16
7. Walther, I., Pippia, P., Meloni, M. A., Turrini, F., Mannu, F., and Cogoli, A. (1998) Simulated microgravity inhibits the genetic expression of interleukin-2 and its receptor in mitogen-activated T lymphocytes. *FEBS Lett.* **436**, 115–118
8. Hughes-Fulford, M. (2003) Function of the cytoskeleton in gravisensing during spaceflight. *Adv. Space Res.* **32**, 1585–1593
9. Unsworth, B. R., and Lelkes, P. I. (1998) Growing tissues in microgravity. *Nat. Med.* **4**, 901–907
10. Hammond, T. G., Lewis, F. C., Goodwin, T. J., Linnehan, R. M., Wolf, D. A., Hire, K. P., Campbell, W. C., Benes, E., O'Reilly, K. C., Globus, R. K., et al. (1999) Gene expression in space. *Nat. Med.* **5**, 359
11. Hoson, T., Kamisaka, S., Masuda, Y., Yamashita, M., and Buchen, B. (1997) Evaluation of the three-dimensional clinostat as a simulator of weightlessness. *Planta* **203**, Suppl., S187–S197
12. Huijser, R. H. (2000) Desktop RPM: new small size microgravity simulator for the bioscience laboratory. In pp. 1–5, Dutch Space, Leiden <http://www.desc.med.vu.nl/Publications/Other/RPM-FS-MG-R00-017.pdf>
14. Quackenbush, J. (2001) Computational analysis of microarray data. *Nat. Rev. Genet.* **2**, 418–427

13. Tjandrawinata, R., Vincent, V., and Hughes-Fulford, M. (1997) Vibrational force alters mRNA expression in osteoblasts. *FASEB J.* **11**, 493–497
15. Irizarry, R. A., Bolstad, B. M., Collin, F., Cope, L. M., Hobbs, B., and Speed, T. P. (2003) Summaries of Affymetrix GeneChip probe level data. *Nucleic Acids Res.* **31**, e15
16. Alizadeh, A. A., Eisen, M. B., Davis, R. E., Ma, C., and Lossos, I. S. (2000) Distinct types of diffuse large B-cell lymphoma identified by gene expression profiling. *Nature* **403**, 503–511
17. Pavlidis, P., and Noble, W. S. (2001) Analysis of strain and regional variation in gene expression in mouse brain. *Genome Biol* **2**, RESEARCH0042
18. Hughes-Fulford, M., Sugano, E., Schopper, T., Li, C. F., Boonyaratanakornkit, J. B., and Cogoli, A. (2005) Early immune response and regulation of IL-2 receptor subunits. *Cell. Signal.* **17**, 1111–1124
19. Eisen, M. B., Spellman, P. T., Brown, P. O., and Botstein, D. (1998) Cluster analysis of genome-wide expression patterns. *Proc. Natl. Acad. Sci. USA* **95**, 14,863–14,868
20. Wingender, E., Chen, X., Fricke, E., Geffers, R., Hehl, R., Liebich, I., Krull, M., Matys, V., Michael, H., Ohnhäuser, R., et al. (2001) The TRANSFAC system on gene expression regulation. *Nucleic Acids Res.* **29**, 281–283
21. Hamalainen, H. K., Tubman, J. C., Vikman, S., Kyrola, T., Ylikoski, E., Warrington, J. A., and Lahesmaa, R. (2001) Identification and validation of endogenous reference genes for expression profiling of T helper cell differentiation by quantitative real-time RT-PCR. *Anal. Biochem.* **299**, 63–70
22. Hatton, J. P., Gaubert, F., Lewis, M. L., Darsel, Y., Ohlmann, P., Cazenave, J. P., and Schmitt, D. (1999) The kinetics of translocation and cellular quantity of protein kinase C in human leukocytes are modified during spaceflight. *FASEB J.* **13**, *Suppl.*, S23–S33
23. Raychaudhuri, S., Stuart, J. M., and Altman, R. B. (2000) Principal components analysis to summarize microarray experiments: application to sporulation time series. *Pac. Symp. Biocomp.* 455–466
24. Li, C., and Wong, W. H. (2001) Model-based analysis of oligonucleotide arrays: expression index computation and outlier detection. *Proc. Natl. Acad. Sci. USA* **98**, 31–36
25. Hawkins, W., and Zieglschmid, J. (1975) Clinical aspects of crew health. In *Biomedical results of Apollo* (Johnston, R., Dietlein, L., and Berry, C., eds) pp. 43-81, NASA, Washington, DC
26. Sciola, L., Cogoli-Greuter, M., Cogoli, A., Spano, A., and Pippia, P. (1999) Influence of microgravity on mitogen binding and cytoskeleton in Jurkat cells. *Adv. Space Res.* **24**, 801–805

27. Hughes-Fulford, M. (2004) Signal transduction and mechanical stress. *Sci. STKE* **249**, RE12
28. Schraven, B., Marie-Cardine, A., Hubener, C., Bruyns, E., and Ding, I. (1999) Integration of receptor-mediated signals in T cells by transmembrane adaptor proteins. *Immunol. Today* **20**, 431–434
29. Zhang, W., and Samelson, L. E. (2000) The role of membrane-associated adaptors in T cell receptor signalling. *Semin. Immunol.* **12**, 35–41
30. Zhong, H., SuYang, H., Erdjument-Bromage, H., Tempst, P., and Ghosh, S. (1997) The transcriptional activity of NF-kappaB is regulated by the IkappaB-associated PKAc subunit through a cyclic AMP-independent mechanism. *Cell* **89**, 413–424
31. Ghosh, S., and Baltimore, D. (1990) Activation in vitro of NF-kappa B by phosphorylation of its inhibitor I kappa B. *Nature* **344**, 678–682
32. Shirakawa, F., and Mizel, S. B. (1989) In vitro activation and nuclear translocation of NF-kappa B catalyzed by cyclic AMP-dependent protein kinase and protein kinase C. *Mol. Cell. Biol.* **9**, 2424–2430
33. Naumann, M., and Scheidereit, C. (1994) Activation of NF-kappa B in vivo is regulated by multiple phosphorylations. *EMBO J.* **13**, 4597–4607
34. Shadduck, R., and Nagabhushanam, N. (1971) Granulocyte colony stimulating factor. I. Response to acute granulocytopenia. *Blood* **38**, 559–568
35. Minami, Y., Kono, T., Miyazaki, T., and Taniguchi, T. (1993) The IL-2 receptor complex: its structure, function, and target genes. *Annu. Rev. Immunol.* **11**, 245–268
36. Cerdan, C., Martin, Y., Courcoul, M., Mawas, C., Birg, F., and Olive, D. (1995) CD28 costimulation regulates long-term expression of the three genes (alpha, beta, gamma) encoding the high-affinity IL2 receptor. *Res. Immunol.* **146**, 164–168
37. Pippia, P., Sciola, L., Cogoli-Greuter, M., Meloni, M. A., Spano, A., and Cogoli, A. (1996) Activation signals of T lymphocytes in microgravity. *J. Biotechnol.* **47**, 215–222
38. Cristillo, A., Macri, M., and Bierer, B. (2003) Differential chemokine expression profiles in human peripheral blood T lymphocytes: dependence on T-cell coreceptor and calcineurin signaling. *Blood* **101**, 216–225
39. Messer, G., Weiss, E. H., and Baeuerle, P. A. (1990) Tumor necrosis factor beta (TNF-beta) induces binding of the NF-kappa B transcription factor to a high-affinity kappa B element in the TNF-beta promoter. *Cytokine* **2**, 389–397
40. Frost, L. L., Neeley, Y. X., Schafer, R., Gibson, L. F., and Barnett, J. B. (2001) Propanil inhibits tumor necrosis factor-alpha production by reducing nuclear levels of the transcription factor nuclear factor-kappaB in the macrophage cell line ic-21. *Toxicol. Appl. Pharmacol.* **172**, 186–193

41. Harrop, J. A., McDonnell, P. C., Brigham-Burke, M., Lyn, S. D., Minton, J., Tan, K. B., Dede, K., Spampanato, J., Silverman, C., Hensley, P., et al. (1998) Herpesvirus entry mediator ligand (HVEM-L), a novel ligand for HVEM/TR2, stimulates proliferation of T cells and inhibits HT29 cell growth. *J. Biol. Chem.* **273**, 27,548–27,556
42. Chan, H., Bartos, D. P., and Owen-Schaub, L. B. (1999) Activation-dependent transcriptional regulation of the human Fas promoter requires NF-kappaB p50-p65 recruitment. *Mol. Cell. Biol.* **19**, 2098–2108
43. Kim, J. O., Kim, H. W., Baek, K. M., and Kang, C. Y. (2003) NF-kappaB and AP-1 regulate activation-dependent CD137 (4-1BB) expression in T cells. *FEBS Lett.* **541**, 163–170
44. Grumont, R., Rourke, I., and Gerondakis, S. (1999) Rel-dependent induction of A1 transcription is required to protect B cells from antigen receptor ligation-induced apoptosis. *Genes Dev.* **13**, 400–411
45. Tixador, R., Richoilley, G., Gasset, G., Planel, H., Moatti, N., Lapchine, L., Enjalbert, L., Raffin, J., Bost, R., Zaloguev, S., et al. (1985) Preliminary results of Cytos 2 experiment. *Acta Astronaut.* **12**, 131–134

Received February 16, 2005; accepted August 24, 2005.

Table 1**Genes up-regulated after early T cell activation in 1 g**

	Expression Ratios			Pathway*	Accession Number
	1 g 0 h	1 g 4 h	vg 4 h		
Apoptosis Induction					
B cell CLL/lymphoma 10 (BCL10)	1	3.3	0.9	NFKB	AF082283
2'-5'-oligoadenylate synthetase 3, 100kDa (OAS3)	1	2.4	5.5	NFKB	NM_006187
Apoptosis Inhibition					
baculoviral IAP repeat-containing 3 (BIRC3)	1	3.8	0.7	NFKB	U37546
BCL2-related protein A1 (BCL2A1)	1	8.8	1.5	CREB; NFKB	NM_004049
TNF receptor-associated factor 1 (TRAF1)	1	5.8	1.2	NFKB	NM_005658
Biosynthesis and Transport					
asparagine synthetase (ASNS)	1	3.2	1.6	ATF; CEBP; SPI	NM_001673
ATPase, Class I, type 8B, member 1 (ATP8B1)	1	2.2	1.4		BG252666
Chediak-Higashi syndrome 1 (CHS1;LYST)	1	2.5	1.1	<i>MYB(-454)</i>	U84744
cytochrome P450, 51 (CYP51)	1	3.7	0.6	CREB; SREB	NM_000786
eukaryotic translation elongation factor 1 epsilon 1 (EEF1E1)	1	2.3	0.5	<i>E2F(-109)</i>	NM_004280
eukaryotic translation initiation factor 2B, subunit 2 β (EIF2B2)	1	4.3	2.8	<i>ELK(-30)</i>	NM_014239
glycyl-tRNA synthetase (GARS)	1	3.1	0.8	<i>E2F(-50)</i>	D30658
JTV1; tRNA synthetase cofactor p38	1	2.6	0.6	<i>CREB(-48)</i>	NM_006303
mitochondrial ribosomal protein L17 (MRPL17)	1	2.1	0.4		AK026857
phosphoribosylaminoimidazole carboxylase (PAICS)	1	3.3	0.8	SP1	AA902652
phosphoserine aminotransferase 1 (PSAT1)	1	2.5	2.0		NM_021154
Sec23 homologue B (<i>S. cerevisiae</i>) (SEC23B)	1	2.7	0.8		BC005032
serine hydroxymethyltransferase 2 (mitochondrial) (SHMT2)	1	2.1	0.7	MYC	AW190316
seryl-tRNA synthetase (SARS)	1	2.5	1.0	<i>ELK(-76)</i>	NM_006513
solute carrier family 3, member 2 (SLC3A2)	1	3.8	1.1	<i>ELK(-44)</i>	NM_002394
solute carrier family 7 member 5 (SLC7A5)	1	3.7	0.7		AB018009
solute carrier family 16 (monocarboxylic acid transporters), member 1 (SLC16A1)	1	2.3	0.6	<i>NFKB(-603)</i>	NM_003051
squalene epoxidase (SQLE)	1	3.3	1.7	SREB	AF098865
tryptophanyl-tRNA synthetase (WARS)	1	5.4	0.9	STAT	NM_004184
Catabolism					
glutamic-oxaloacetic transaminase 2, mitochondrial (GOT2)	1	2.8	0.9	CEBP	NM_002080
hexokinase (HK2)	1	2.5	0.3	CREB	AI761561
Cell Cycle Regulation and DNA Replication and Repair					
BTG family, member 3 (BTG3)	1	3.8	1.1		NM_006806
cyclin-dependent kinase 4 (CDK4)	1	2.1	0.9	MYC	NM_000075
KIN, antigenic determinant of recA protein homologue (mouse) (KIN)	1	3.3	0.6		NM_012311
MAD2 mitotic arrest deficient-like 1 (MAD2L1)	1	2.9	0.9	<i>ELK(-654)</i>	NM_002358
retinoblastoma binding protein 8 (RBBP8)	1	3.8	2.3		NM_002894
serine/threonine kinase 12 (STK12;AURKB)	1	6.1	14.2	E2F	AB011446
Cell Structure, Nuclear, and Cytoskeletal Maintenance					
dynactin 4 (DCTN4)	1	2.6	2.2	<i>CREB(-85); SREB(-24)</i>	NM_016211
H3 histone family, member B (HIST1H3D)	1	3.3	52.0	NFKB	NM_003530
thyroid hormone receptor interactor 10 (TRIP10) [†]	1	2.0	1.5	<i>E2F(-919); NFKB(-892)</i>	NM_004240

Cell Adhesion and Cell Communication

selectin L (SELL)	1	2.7	0.5	NFKB	NM_000655
-------------------	---	-----	-----	------	-----------

Cytokines, Chemokines, and Growth Factors

chemokine (C motif) ligand 1 (XCL1)	1	26.6	1.7	NFAT	NM_002995
chemokine (C motif) ligand 2 (XCL2)	1	252.0	8.4	NFAT	NM_003175
chemokine (C-C motif) ligand 3 (CCL3)	1	7.8	0.8	AP1; CEBP; NFAT	NM_002983
chemokine (C-C motif) ligand 4 (CCL4)	1	29.5	2.6	CREB; NFKB	NM_002984
chemokine (C-C motif) ligand 20 (CCL20; MIP3A)	1	61.3	0.6	NFKB	NM_004591
chemokine (C-X-C motif) ligand 10 (CXCL10)	1	10.0	2.1	NFKB; STAT	NM_001565
colony stimulating factor 2 (granulocyte-macrophage) (CSF2)	1	88.5	1.8	NFKB; STAT	M11734
interferon, gamma (IFNG)	1	82.6	6.3	NFKB; STAT	M29383
interleukin 1 family, member 9 (IL1F9)	1	5.6	3.1	AP1; NFKB	NM_019618
interleukin 2 (IL2) [†]	1	83.3	6.8	AP1; CREB; NFAT; NFKB; STAT	NM_000586
lymphotoxin- α (LTA; TNFSF1)	1	99.7	3.9	NFKB	NM_000595
macrophage migration inhibitory factor (glycosylation-inhibiting factor) (MIF)	1	2.8	0.4	AP1; CREB	NM_002415
tumor necrosis factor (ligand) superfamily, member 14 (TNFSF14)	1	6.4	1.6	AP1; NFAT; NFKB	NM_003807
tumor necrosis factor (TNF Superfamily, Member 2) (TNF; TNFA)	1	29.7	2.3	AP1; CREB; NFAT; NFKB	NM_000594

Cytokine, Chemokine, and Growth Factor Receptors

interleukin 2 receptor, α (IL2RA)	1	10.9	2.0	STAT	K03122
killer cell immunoglobulin-like receptor, three domains, long cytoplasmic tail, 2 (KIR3DL2)	1	3.8	2.7	<i>E2F(-50)</i>	AF022048
tumor necrosis factor receptor superfamily, member 6 (TNFRSF6; FAS antigen)	1	2.1	1.0	AP1; CEBP; NFKB; p53; SP1; STAT	AA164751
tumor necrosis factor receptor superfamily, member 9 (TNFRSF9)	1	7.5	0.8	AP1; NFKB	NM_001561

Signal Transduction

CD59 antigen p18-20 (CD59)	1	3.4	0.7	p53	X16447
dual specificity phosphatase 5 (DUSP5)	1	12.8	0.8	ELK	U16996
non-metastatic cells 1 (NME1)	1	5.4	0.9	<i>ELK(-136)</i>	NM_000269
non-metastatic cells 2 (NME2)	1	3.4	1.0	<i>ELK(-213)</i>	NM_002512
phosphoprotein enriched in astrocytes 15 (PEA15)	1	3.2	1.2	ELK	NM_003768
sel-1 suppressor of lin-12-like (SEL1L)	1	2.1	0.7		AI927770
SLAM family member 7 (SLAMF7; CRACC)	1	3.0	1.7		NM_021181
serine/threonine kinase 3 (STE20 homologue, yeast) (STK3)	1	17.4	11.1		NM_006281

Immediate Early Response (IER)

early growth response 1 (Krox-24) (EGR1)	1	5.5	3.2	CREB; NFKB	NM_001964
early growth response 2 (Krox-20 homologue, Drosophila) (EGR2)	1	8.9	1.0	CREB	NM_000399
immediate early response 3 (IER3)	1	15.0	1.5	NFKB	NM_003897

Transcription

aryl hydrocarbon receptor (AHR)	1	2.8	0.2	CREB	NM_001621
cAMP responsive element binding protein 1 (CREB1)	1	2.2	1.2	CREB; NFKB	AA161486
CD3-epsilon-associated protein; antisense to ERCC-1 (ASE-1)	1	12.9	2.8		NM_012099
E2F transcription factor 6 (E2F6)	1	2.9	0.6	E2F	NM_001952
enhancer of zeste homologue 2 (EZH2)	1	8.4	0.7	E2F; RB	NM_004456
interferon regulatory factor 4 (IRF4)	1	6.1	3.3	NFKB	D78261
v-maf musculoaponeurotic fibrosarcoma oncogene homologue F (avian) (MAFF)	1	9.8	1.6	CREB	AL021977
nuclear factor (erythroid-derived 2)-like 3 (NFE2L3)	1	2.7	0.9		NM_004289
nuclear factor of kappa light polypeptide gene enhancer in B-cells 1 (NFKB1)	1	4.9	1.2	NFKB	M55643

nucleolar and coiled-body phosphoprotein 1 (NOLC1)	1	3.9	1.0	CREB	NM_004741
signal transducer and activator of transcription 1 (STAT1) (control sequence)	1	10.8	3.8	STAT	M97935
signal transducer and activator of transcription 1, 91kDa (STAT1)	1	7.6	1.7	STAT	NM_007315
v-myb myeloblastosis viral oncogene homologue (myb)	1	2.9	0.9	E2F	NM_005375

RNA Processing and Turnover

ATP/GTP binding protein (HEAB)	1	2.5	1.0		NM_006831
DEAD/H (Asp-Glu-Ala-Asp/His) box polypeptide 24 (DDX24)	1	2.7	1.1		NM_020414
EBNA1 binding protein 2 (EBNA1BP2)	1	3.1	0.6	<i>ELK(-56; -62; -81)</i>	NM_006824
heterogeneous nuclear ribonucleoprotein A/B (HNRPA)	1	2.7	0.5		NM_004499
U3 snoRNP-associated 55-kDa protein (RNU3IP2; U3-55K)	1	11.8	2.2	<i>ELK(-233)</i>	NM_004704

Protein Processing and Turnover

a disintegrin and metalloproteinase domain 17 (tumor necrosis factor, α , converting enzyme) (ADAM17)	1	8.3	3.9	<i>ELK(-57; -91)</i>	U86755
F-box only protein 9 (FBXO9)	1	2.5	1.6	<i>REL(-288)</i>	AI954041
Homo sapiens cDNA FLJ36423 fis, clone THYMU2011308 (CAPN7)	1	2.8	2.4	<i>NFE2(-700)</i>	BE349584
matrix metalloproteinase 1 (interstitial collagenase) (MMP1)	1	27.2	8.3	AP1; NFKB; STAT	NM_002421
proteasome (prosome macropain) subunit, α type, 3 (PSMA3)	1	2.3	0.7		NM_002788
proteasome (prosome macropain) subunit, β type, 5 (PSMB5)	1	2.4	0.4	<i>API(-284); ELK(-280)</i>	BC004146
proteasome (prosome, macropain) 26S subunit, ATPase, 4 (PSMC4)	1	3.4	0.8	<i>MYB(-29)</i>	NM_006503
proteasome (prosome, macropain) 26S subunit, non-ATPase, 5 (PSMD5)	1	2.3	0.9	<i>MYB(-355)</i>	AU157008
serine (or cysteine) proteinase inhibitor, clade E, member 2 (SERPINE2)	1	4.2	1.3	<i>MYB(-848)</i>	AL541302
seven in absentia homologue 2 (Drosophila) (SIAH2)	1	6.7	1.1	<i>API(-460)</i>	U76248
stromal cell-derived factor 2-like 1 (SDF2L1)	1	2.3	1.1		NM_022044

Unclear Function or Role in Cellular Processes

CGI-07	1	2.9	2.9	<i>ELK(-516)</i>	NM_015938
class-I MHC-restricted T cell associated molecule (CRTAM)	1	44.0	5.5		NM_019604
retinoic acid induced 2 (RAI2)	1	4.3	5.2		NM_021785
small EDRK-rich factor 2 (SERF2)	1	2.7	0.9		NM_005770
TRK-fused gene (TFG)	1	2.1	0.9	<i>ELK(-176)</i>	NM_006070

Bold numbers indicate significant differential expression as measured by a paired *t* test ($P \leq 0.05$) relative to 1 g 0 h. *Gene is either directly involved in signal transduction through the transcription factor or is transcriptionally regulated by the transcription factor. †Paired *t* test *P* value was 0.0514 due to an especially high increase in expression by T cells from 1 donor after activation in normal gravity. However, IL2 is included here, because its expression profile was confirmed by quantitative RT-PCR. *Italics* indicate the presence of a putative transcription factor binding site. Numbers in parentheses correspond to farthest distance of consensus sequence from transcription start site on strand coding the gene.

Fig. 1

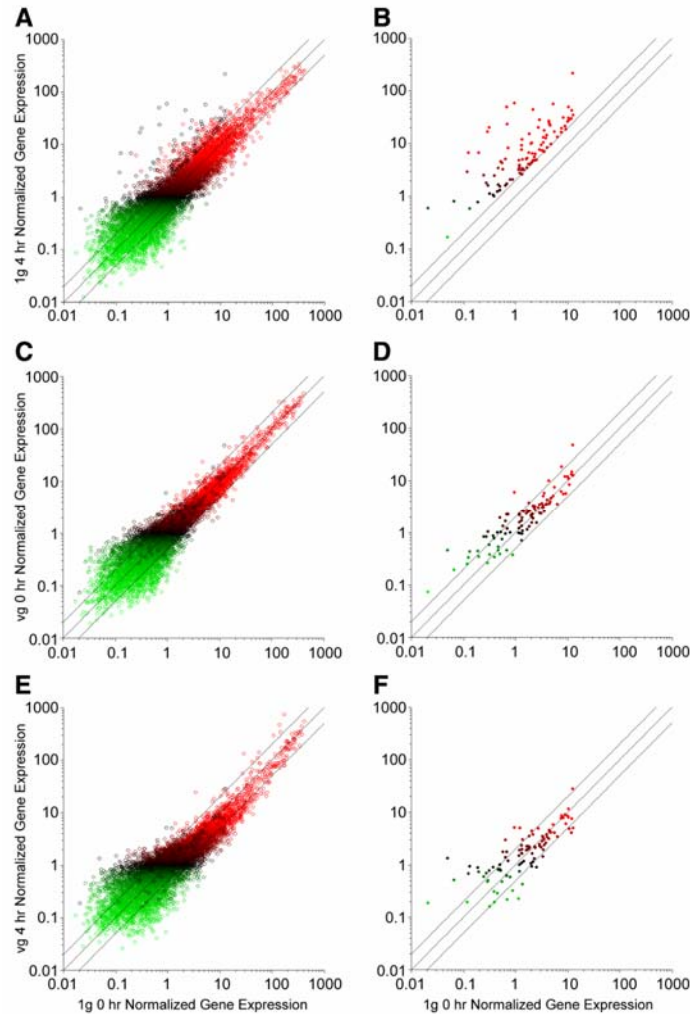


Figure 1. Gravity-dependent distribution of gene expression during human T cell activation. **A)** Plot of normalized gene expression, from the average of 3 donors, during T cell activation on ground at 1 g compared with corresponding expression in unactivated T cells at 1 g. **B)** Plot of expression at 1 g 4 h of filtered genes significantly up-regulated after activation. **C)** Plot of normalized gene expression from untreated T cells cultured on RPM. **D)** Plot of expression from untreated T cells on the RPM for filtered genes. **E)** Plot of expression from T cells treated with Con A and anti-CD28 antibody for 4 h on RPM. **F)** Plot of expression from treated T cells on RPM for filtered genes; 2 outer diagonals in each scatter plot represent a 2-fold change boundary, while central diagonal represents equivalent expression ratios across conditions compared. Red represents gene expression above chip median, while green represents expression below median. In plots showing all genes, black represents filtered genes.

Fig. 2

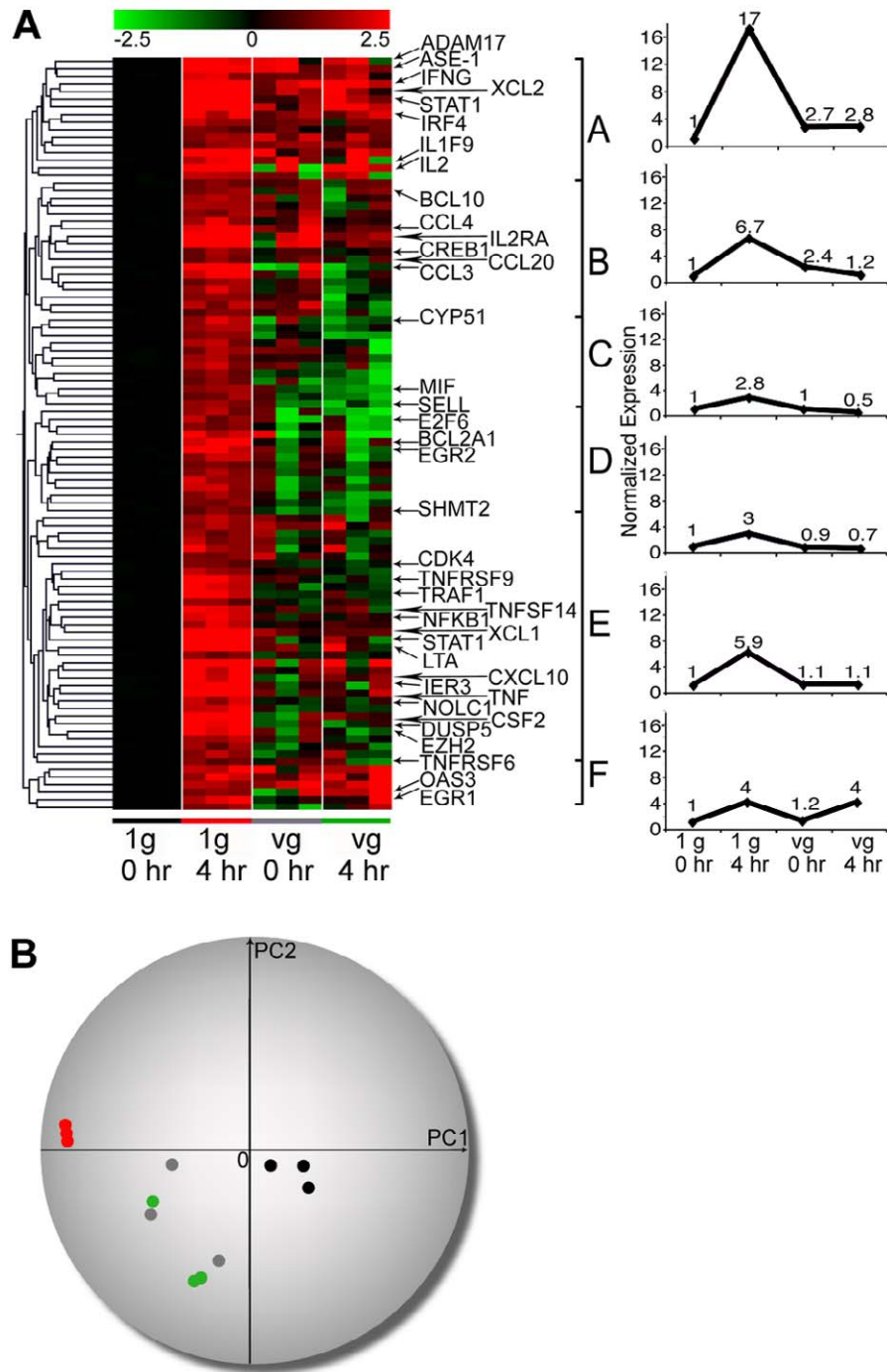


Figure 2. Cluster analysis of 12 samples and 99 genes from T cells activated at 1 g or on RPM. **A)** We used a centered Pearson correlation as distance metric to sort data and group genes based on mathematical distance between expression profiles. A single row of colored boxes represents each gene, while columns represent experiment profiles for 12 T cell samples. Genes that appear more than once reflect multiple probe sets on array that target same sequence or a different sequence in same UniGene cluster. Color scale ranges from green, for down-regulation, to red, for up-regulation in \log_2 scale. Expression profiles from average signals of genes for each condition in each of 6 clusters are shown at **right**. **B)** Principal component analysis on 12 samples using 2 principal components as x and y axes. Unactivated T cells at 1 g are shown in black, activated T cells at 1 g are shown in red, unactivated T cells in vg are shown in gray, and activated T cells in vg are shown in green.

Fig. 3

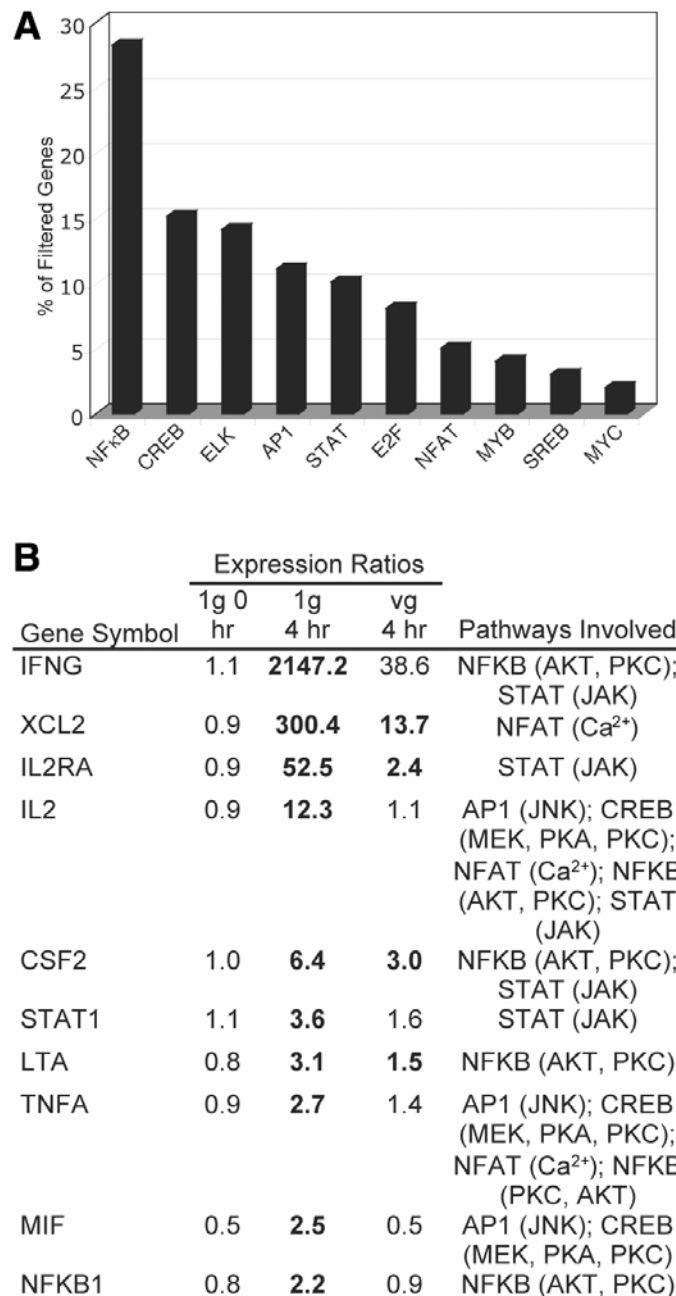


Figure 3. Functional and regulatory classification of genes after T cell activation in normal gravity. We extensively examined published literature and annotations associated with significant genes to search for common regulatory elements and function and ranked these elements according to their frequency of occurrence. **A)** Percent abundance of these genes was examined based on common transcription factor binding sites or pathway involvement. **B)** Expression profiles of 10 genes identified by microarray analysis as integral to effective T cell mediated immune response were validated by real-time RT-PCR. Bold numbers indicate significant differential expression relative to 1 g 0 h as measured by using an unpaired 1-tailed Student's *t* test ($P \leq 0.05$) on technical triplicate samples to test for significant up-regulation.

Fig. 4

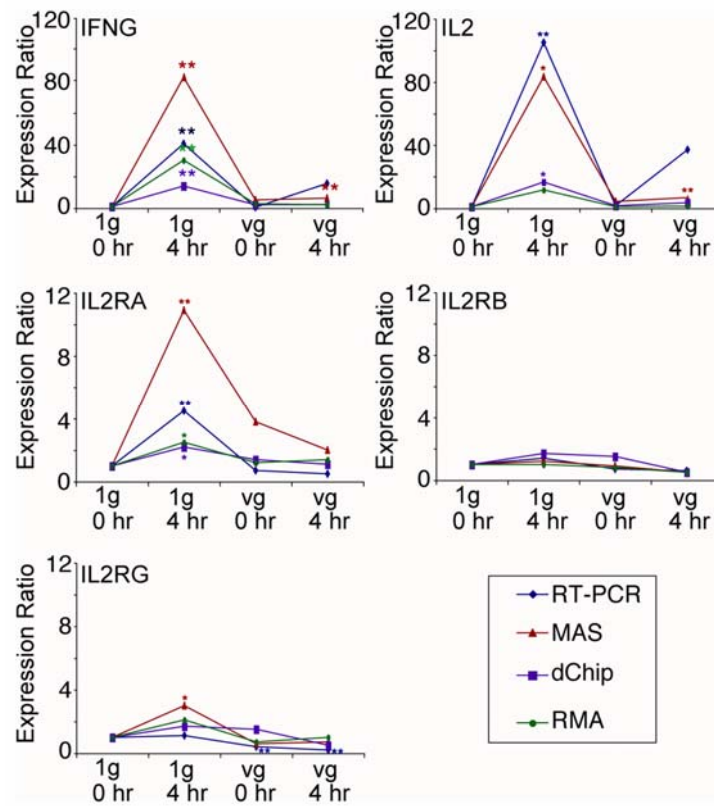


Figure 4. Microarray and RT-PCR analyses confirm expression profiles for *IFNG*, *IL2*, *IL2RA*, *IL2RB*, and *IL2RG*. Average normalized expression ratios from MAS, dChip, and RMA preprocessed data and semiquantitative RT-PCR data for these 5 genes are shown. *Significant differential gene expression compared with expression at 1 g 0 h from a paired two-tailed *t* test on logarithms of normalized signals with $P \leq 0.05$. **Significant differential gene expression with $P \leq 0.01$. A sample size of 3 was available for microarray analysis. T cell samples from each donor were split to create 4 independent biological replicates. Thus, statistical tests for semi-quantitative RT-PCR were performed on a sample size of 12.

Fig. 5

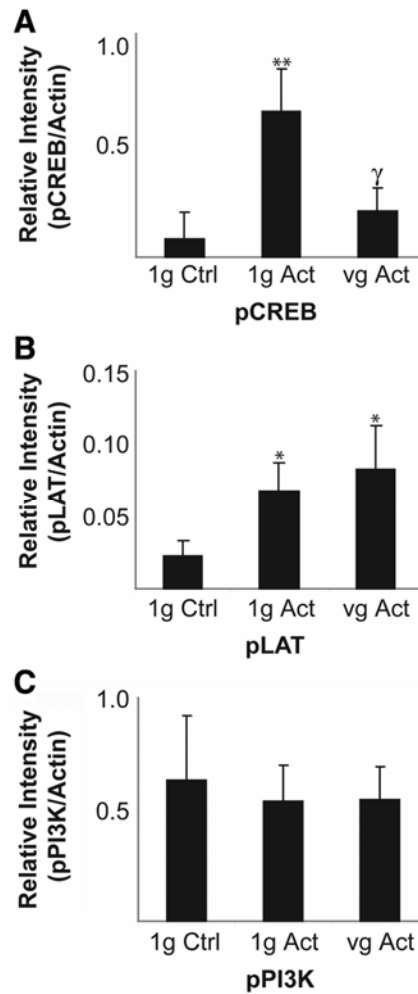


Figure 5. Mitogenic T cell activation leads to CREB and LAT phosphorylation in 1 g, while CREB phosphorylation is suppressed in vg. **A)** T cell activation (Act) with Con A and anti-CD28 leads to CREB phosphorylation in 1 g but not in vg. **B)** T cell activation with Con A and anti-CD28 leads to comparable LAT phosphorylation in both 1 g and vg compared with unactivated controls (Ctrl). **C)** No significant changes in PI3-K phosphorylation occur by 30 min of mitogen treatment in 1 g and vg. Buffy coat isolated peripheral T cells were subjected to 5 $\mu\text{g/ml}$ Con A and 4 $\mu\text{g/ml}$ anti-CD28 antibody. Thirty minutes after activation, total protein was isolated and Western blot was performed against anti-phospho-CREB (Ser133), anti-phospho-LAT (Tyr171), and anti-phospho-PI3-K (Tyr508) antibodies. Each band was normalized to internal actin standard. Bars show mean \pm SD ($n=4$). * $P < 0.01$ and ** $P < 0.001$ against 1 g control. $\gamma P < 0.01$ against 1 g activated samples.

